

Hepatic Bipolar Radio-Frequency Ablation Between Separated Multiprong Electrodes

Dieter Haemmerich, *Student Member, IEEE*, S. Tyler Staelin, Supan Tungjitkusolmun, *Member, IEEE*, Fred T. Lee, Jr., David M. Mahvi, and John G. Webster*, *Life Fellow, IEEE*

Abstract—Radio-frequency (RF) ablation has become an important means of treatment of nonresectable primary and metastatic liver tumors. Major limitations are small lesion size, which make multiple applications necessary, and incomplete killing of tumor cells, resulting in high recurrence rates. We examined a new bipolar RF ablation method incorporating two probes with hooked electrodes (RITA model 30). We performed monopolar and bipolar *in vivo* experiments on three pigs. The electrodes were 2.5 cm apart and rotated 45° relative to each other. We used temperature-controlled mode at 95 °C. Lesion volumes were $3.9 \pm 1.8 \text{ cm}^3$ ($n = 7$) for the monopolar case and $12.2 \pm 3 \text{ cm}^3$ ($n = 10$) for the bipolar case. We generated finite-element models (FEMs) of monopolar and bipolar configurations. We analyzed the distribution of temperature and electric field of the finite element model. The lesion volumes for the FEM are 7.95 cm^3 for the monopolar and 18.79 cm^3 for the bipolar case. The new bipolar method creates larger lesions and is less dependent on local inhomogeneities in liver tissue—such as blood perfusion—compared with monopolar RF ablation. A limitation of the new method is that the power dissipation of the two probes cannot be controlled independently in response to different conditions in the vicinity of each probe. This may result in nonuniform lesions and decreased lesion size.

Index Terms—Bipolar ablation, electrode, finite element model, liver ablation, radio-frequency, RF ablation.

I. INTRODUCTION

RADIO-FREQUENCY (RF) ablation has become of considerable interest as a minimally invasive treatment for primary and metastatic liver tumors. *Hepatocellular carcinoma* is one of the most common malignancies, worldwide with an estimated annual mortality of 1 000 000 people [1]. Surgical resection offers the best chance of long-term survival, but is rarely possible. In many patients with cirrhosis or with multiple tumors, hepatic reserve is inadequate to tolerate resection and alternative means of treatment are necessary [2]. In RF

ablation, RF current is delivered to the tissue via electrodes inserted percutaneously or during surgery. Different modes of controlling the electromagnetic power delivered to tissue can be utilized. Power-controlled mode ($P = \text{constant}$), temperature-controlled mode ($T = \text{constant}$) and impedance-controlled mode ($Z < \text{constant}$) are commonly used. The electromagnetic energy is converted to heat by ionic agitation. Temperatures above 45 °C–50 °C have been shown to cause denaturation of intracellular proteins and destruction of membranes of tumor cells, eventually resulting in cell *necrosis* [3]. One of the major limitations of this technique is the extent of induced *necrosis*. When tumors greater than 2 cm are treated, multiple applications are necessary to obtain complete tumor *necrosis*. Often tumor cells survive, which leads to high recurrence rates [4]–[7]. Several methods have been investigated for increasing lesion size and improving efficacy. Internally cooled probes have been used [8], [9]. Pulsed techniques have been used to further increase *necrosis* diameter created by internally cooled probes [10]. *Interstitial* saline infusion creates larger lesions by cooling and increasing effective electrode area [11]–[13]. The cooling effects of large blood vessels and *vascular* perfusion can be minimized by the Pringle maneuver, in which *vascular* inflow occlusion is performed by clamping the hepatic artery and portal vein [14]. However, the Pringle requires a major surgical procedure, which negates one of the major advantages of RF ablation—the use in a minimally invasive fashion (percutaneous or laparoscopic). Vasoactive pharmacologic agents have also been used to reduce blood flow to the liver [15] to reduce the blood cooling effect.

Bipolar RF ablation has been shown to create larger lesions using two-needle electrodes compared with monopolar ablation using a single-needle electrode [2], [13], [16]. We investigated the potential of a novel bipolar RF ablation technique using two parallel oriented, hooked electrodes (model 30, RITA Medical Systems, Mountain View, CA). There have been many finite-element method (FEM) studies of cardiac RF ablation [17], [18] but few FEM modeling studies on hepatic ablation [19]. We initially generated FEM models to analyze differences in distribution of temperature and electric field intensity. We created monopolar and bipolar lesions *in vivo* in pig liver and compared the results with the FEM model.

II. MATERIALS AND METHODS

We used a RITA 500 RF generator and RITA 4-prong 15-gauge probes (model 30, RITA Medical Systems, see Fig. 1) for creating monopolar and bipolar lesions. For clinical use,

Manuscript received September 28, 2000; revised July 2, 2001. This work was supported by the National Institutes of Health (NIH) under Grant HL56143. Asterisk indicates corresponding author.

D. Haemmerich is with the Department of Biomedical Engineering, University of Wisconsin, Madison, WI 53706 USA.

S. T. Staelin and D. M. Mahvi are with the Department of Surgery, University of Wisconsin, Madison, WI 53792 USA.

S. Tungjitkusolmun is with the Department of Electronics Engineering, King Mongkut's Institute of Technology Ladkrabang, Chalokkrung Rd., Ladkrabang, Bangkok, 10520, Thailand.

F. T. Lee, Jr., is with the Department of Radiology, University of Wisconsin, Madison, WI 53792 USA.

*J. G. Webster is with the Department of Biomedical Engineering, University of Wisconsin, 1415 Engineering Drive, Madison, WI 53706 USA (e-mail: webster@engr.wisc.edu).

Publisher Item Identifier S 0018-9294(01)08279-9.

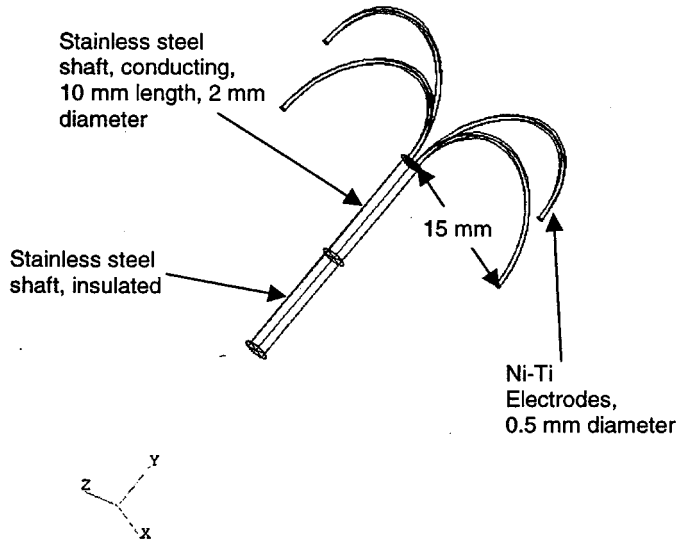


Fig. 1. Geometry of fully deployed Rita model 30 umbrella probe used in FEM. The prongs and the distal 10 mm of the shaft conduct RF current. The orientation of the coordinates is shown at the bottom.

the probe is inserted with retracted prongs. Once the probe is in place, the prongs are deployed. The prongs can be deployed to a maximum diameter of 3 cm. A thermistor is located in the tip of each of the prongs. The thermistors allow temperature monitoring with an accuracy of $\pm 2^\circ\text{C}$ from 35°C to 100°C and $\pm 5^\circ\text{C}$ over 100°C . The shaft of the probe is insulated to within 1 cm of the tip. For creating bipolar lesions, we attached a second probe to the generator replacing the dispersive electrode using a modified cable for connection. Figs. 2 and 3 show the electrical configuration for monopolar and bipolar ablation, respectively. The control circuit varies the applied power so that the temperature, which is monitored by the thermistors, is kept constant.

A. Bioheat Equation

Joule heating arises when an electric current passes through a conductor. Electromagnetic energy is converted into heat. The heating of tissue during RF ablation is governed by the bioheat equation:

$$\rho c \frac{\partial T}{\partial t} = \nabla \cdot k \nabla T + \mathbf{J} \cdot \mathbf{E} - h_{bl}(T - T_{bl}) - Q_m$$

$$h_{bl} = \rho_{bl} c_{bl} w_{bl}$$

where

ρ	density (kg/m^3);
c	specific heat ($\text{J}/\text{kg}\cdot\text{K}$);
k	thermal conductivity ($\text{W}/\text{m}\cdot\text{K}$);
J	current density (A/m^2);
E	electric field intensity (V/m);
T_{bl}	temperature of blood;
ρ_{bl}	blood density (kg/m^3);
c_{bl}	specific heat of the blood ($\text{J}/\text{kg}\cdot\text{K}$);
w_{bl}	blood perfusion (L/s);
h_{bl}	convective heat transfer coefficient accounting for the blood perfusion;

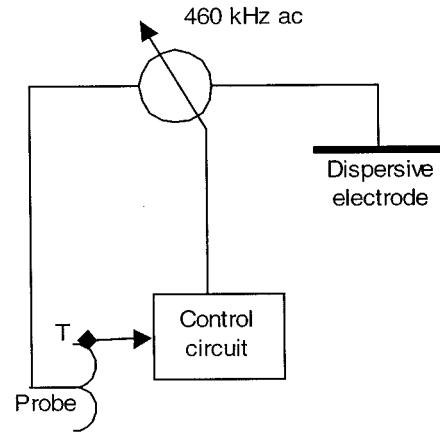


Fig. 2. Electrical configuration of monopolar ablation.

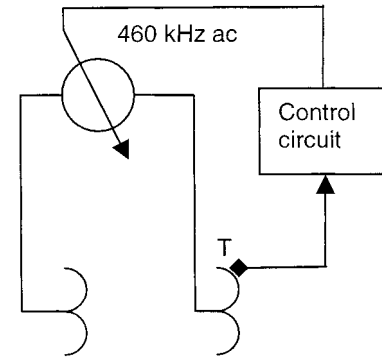


Fig. 3. Electrical configuration of bipolar ablation.

Q_m (W/m^3) energy generated by metabolic processes and was neglected since it is small compared with the other terms.

In the Pennes model described in the bioheat equation, the energy exchange between blood and tissue is modeled as a nondirectional heat source. One major assumption is that the heat transfer related to perfusion between tissue and blood occurs in the capillary bed, which turned out not to be fully correct. The main thermal equilibrium process takes place in the precapillary or postcapillary vessels. Nevertheless, the Pennes model describes blood perfusion with acceptable accuracy, if no large vessels are nearby [20]. The blood perfusion in hepatic tissue used in the FEM was $w_{bl} = 6.4 \times 10^{-3}$ [21].

B. Finite-Element Method

We created FEM models for monopolar and bipolar ablation. For all FEM analyses, we used a RITA model 30, 4-prong probe. Initially we created different FEM models for bipolar ablation where we varied probe distance in 0.5-cm increments. We found the ideal distance (i.e., largest lesion size) at 2-cm probe distance.

Fig. 1 shows the geometry of the probe model. For the bipolar model, the distal probe shaft was considered insulated, except for the most distal 2 mm. In the actual probe, the shaft tip is cut at an angle. Even though we insulated the outside of the shaft, the inside still conducts and contributes toward lesion formation. We created a similar situation in the model by considering the distal 2 mm of the distal probe conducting.

TABLE I
MATERIAL PROPERTIES USED IN FEM

Element	Material	ρ [kg/m ³]	c [J/kg·K]	k [W/m·K]	σ [S/m]
Electrode	Ni-Ti	6450	840	18	1×10^8
Shaft	Stainless steel	21500	132	71	4×10^6
Tissue	Liver	1060	3600	0.512	0.333

The probes were placed within a cylinder (80-mm diameter) of liver tissue in this formation. Due to the symmetry of the arrangement, we could reduce computing time by only modeling a quarter of the cylinder. Table I lists the material properties used in the model, which were taken from the literature [22], [23]. We set the initial temperature of the liver tissue and temperature at the boundary of the model to 37 °C. Blood perfusion was modeled according to the Pennes model [24]. We simulated ablation for 12 min. The maximum temperature of hepatic tissue was kept at 95 °C by varying the voltage applied to the electrodes. The lesion size was determined using the 50 °C margin (i.e., tissue above 50 °C is considered destroyed). The bipolar model consisted of $\sim 63\,000$ tetrahedral elements and $\sim 12\,000$ nodes. The monopolar model consisted of $\sim 35\,000$ tetrahedral elements and ~ 7000 nodes. We used PATRAN Version 9.0 (The MacNeal-Schwendler Co., Los Angeles, CA) to generate the geometric models, assign material properties, assign boundary conditions and perform meshing. After creating the model, PATRAN generates an input file for the ABAQUS/Standard 5.8 (Hibbitt, Karlsson & Sorensen, Inc., Pawtucket, RI) solver. A coupled thermo-electrical analysis was performed by ABAQUS. For postprocessing we used the built-in module ABAQUS/POST to generate profiles of temperature and electric field intensity. All analysis was performed on a HP-C180 workstation equipped with 1.1 GB of RAM and 34 GB of hard disk space. Tungjitkusolmun *et al.* [17] provide a detailed description of the FE modeling process.

C. In Vivo Studies

We used three domestic pigs (30–40 kg) for the *in vivo* experiments. We obtained preapproval for all animal experiments from the Institutional Animal Care and Use Committee, University of Wisconsin, Madison. All procedures were performed with the animals under general *anesthesia*. Induction of *anesthesia* was achieved by using an *intramuscular* injection of tiletamine hydrochloride, zolazepam hydrochloride, and xylazine hydrochloride. The animals were then intubated and maintained on inhaled halothane. Once adequate *anesthesia* was achieved, the *abdomen* was opened. The placement of the electrodes was guided by ultrasonic imaging to avoid blood vessel rupture and placement near large vessels. The probes were inserted with retracted prongs. The prongs were deployed once the probes were placed at the desired position. For monopolar ablations, the dispersive electrode was placed on the subject's back *posterior* to the liver. We performed preliminary *in vivo* experiments with bipolar configuration at probe distances of 3.5, 3, and 2.5 cm. When the distance was 3.5 and 3 cm, in some cases we found a gap of viable tissue between two lesions created by the two probes after performing ablation. Subsequently, probes were placed 2.5 cm apart. Furthermore, probes were rotated 45° relative to each other, and no dispersive electrode was

used. The distal 10 mm of the distal probe shaft were insulated using epoxy resin (see Fig. 4). Both monopolar and bipolar ablations were performed for 12 min using temperature-controlled mode at 95 °C. After the experiments were completed, the animal was sacrificed and the ablated liver lobes were resected. The liver was placed in 10% formalin for fixation. After fixation, the tissue was cut into slices 3–5 mm thick and the slices were scanned at a resolution of 300 dpi to obtain digital images. We measured the lesion area of each slice using the software ImageJ Version 1.16 (NIH). The lesion border was determined by optical inspection. The pale central area of the RF lesion has been shown to correspond to the zone of *necrosis* [25]. Lesion volume was computed by multiplying the lesion area of each slice by slice thickness, and summing results for all slices.

III. RESULTS

A. In Vivo Studies

We created seven monopolar and ten bipolar lesions. Tables II and III show the lesion volumes of the resulting bipolar and monopolar lesions respectively. For monopolar ablation, lesion volumes were 3.9 ± 1.8 cm³. For bipolar ablation, lesion volumes were 12.2 ± 3 cm³. Figs. 5 and 6 show typical monopolar and bipolar lesions, respectively. Fig. 7 shows a bipolar lesion with severe charring around the shaft of the distal probe. Fig. 8 shows a bipolar lesion where the two probes have been heated nonuniformly.

B. Finite Element Method

We generated models of monopolar and bipolar ablation and analyzed the distribution of temperature and electric field intensity. Figs. 9 and 10 show the profiles of the temperature distributions of monopolar and bipolar ablation, respectively. The lesion volumes were 7.95 cm³ for monopolar ablation and 18.79 cm³ for bipolar ablation. The monopolar model shows a mushroom shaped lesion while the bipolar model resembles the shape of a cylinder. Figs. 11 and 12 show the electric field intensity of monopolar and bipolar ablation, respectively.

IV. DISCUSSION

We propose a new bipolar method for creating larger and more controllable lesions (i.e., less dependent on local inhomogeneities in liver tissue such as blood perfusion).

In the bioheat equation, the term $J \cdot E$ represents the power density p of the electromagnetic field, which is converted into thermal energy. The electric field intensity E can be expressed as $E = J \cdot \rho$, where ρ is the electric resistivity. Therefore, the power density can also be expressed as $p = E^2/\rho$. Fig. 11 shows that the electric field intensity is high only very close to the probe; hence, active heating is also limited to this region. We hypothesized that we could extend the zone of high field intensity further away from the probe using the bipolar configuration and thereby extend the zone of active heating.

In the ideal case of two parallel plates at different voltages extending infinitely in all directions, electric field intensity is homogenous. Then, the deposition of electric energy is homogenous, if the electrical resistivity of the material in between

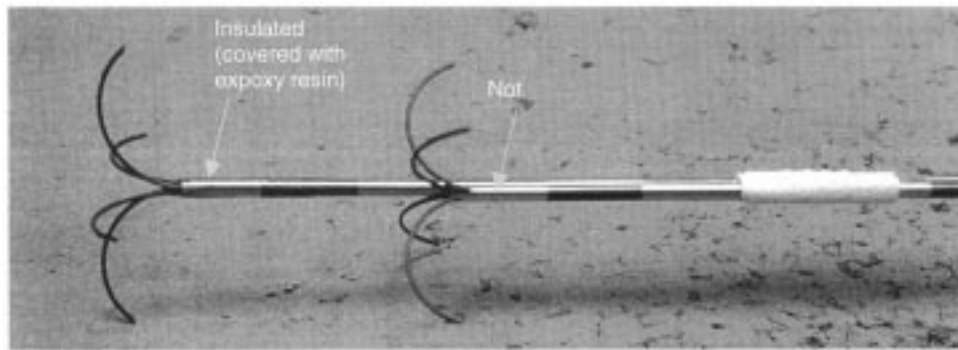


Fig. 4. Arrangement of two probes for bipolar ablation.

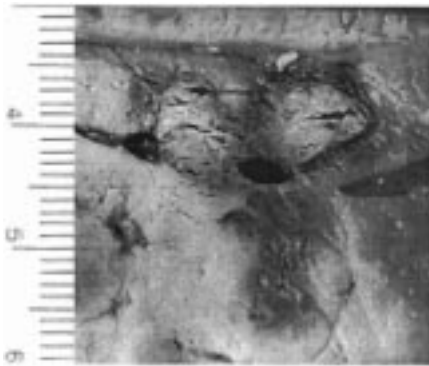


Fig. 5. *In vivo* monopolar lesion. Lesion volume $V = 3.0 \text{ cm}^3$.

TABLE II
LESION SIZES, *IN-VIVO*, BIPOLAR ABLATION

Lesion #	Subject #	Lesion Volume (cm^3)
1	1	14.2
2	1	10.3
3	1	16.8
4	2	13.8
5	2	8.3
6	2	14.5
7	3	11.6
8	3	12.2
9	3	13.4
10	3	6.9
Average (StdDev.)		12.2 (± 3)

TABLE III
LESION SIZES, *IN-VIVO*, MONOPOLAR ABLATION

Lesion #	Subject #	Lesion Volume (cm^3)
1	1	6.9
2	2	3.1
3	2	2.5
4	2	3.5
5	2	3.0
6	3	6.1
7	3	2.5
Average (StdDev.)		3.9 (± 1.8)

the plates is constant. When the plates have finite dimensions and the distance between the plates is small compared with the plate dimensions, a homogenous electric field gradient develops

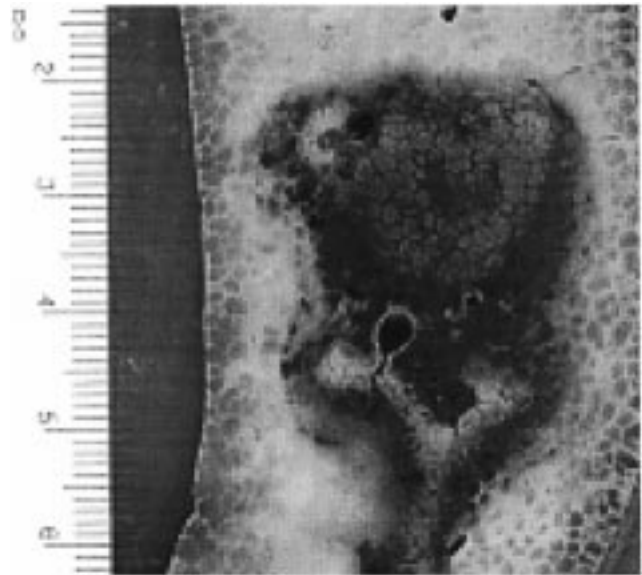


Fig. 6. *In vivo* bipolar lesion. Lesion volume $V = 14.2 \text{ cm}^3$.

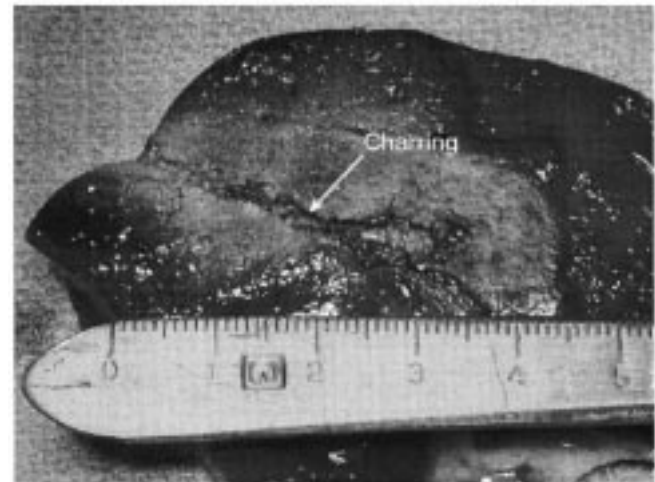


Fig. 7. *In vivo* bipolar lesion, severe charring around uninsulated shaft of distal probe, lesion volume $V = 12.2 \text{ cm}^3$.

in-between the plates except for the plate edges. Fig. 13 shows this situation for the electric field gradient of two plates. We tried to create a similar case by using two umbrella electrodes placed parallel to each other at a close distance. We examined the electric field between two such probes with a FEM model. Figs. 11



Fig. 8. Nonuniform heating. Lower probe creates smaller lesion due to lower temperature. Lesion volume $V = 10.3 \text{ cm}^3$.

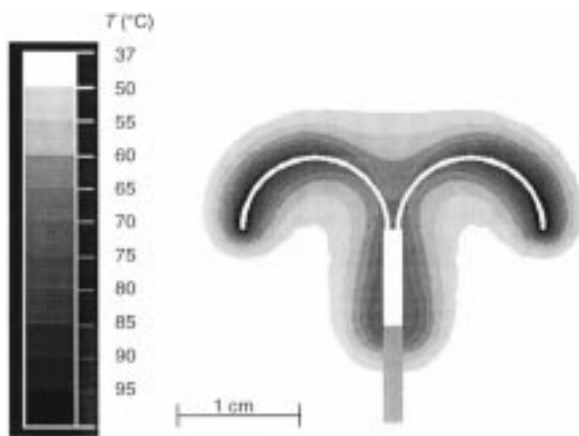


Fig. 9. Monopolar RF ablation: Temperature distribution after 12 min RF ablation in temperature-controlled mode, $T = 95 \text{ }^\circ\text{C}$. The distal 10 mm of the shaft and the prongs conduct current. The gray part of the shaft is insulated. The outermost border (lightest gray) marks the $50 \text{ }^\circ\text{C}$ margin, which is considered the lesion border. Lesion size $V = 7.95 \text{ cm}^3$.

and 12 show the electric field intensity for the monopolar and bipolar configurations. For the bipolar configuration we see increased field intensity between the probes. However, for probes with four prongs this increase is not sufficient to contribute significantly toward heating (note the scale, where the shades of gray correspond to field intensity from zero to 1/3 of the maximum intensity). Black covers the range above 1/3 of maximum field intensity). Therefore, probes with a large number of prongs are necessary for the heating between probes to become considerable. Disadvantages of using probes with a higher number of prongs are increased risk of blood vessel rupture and the necessity for a larger gauge needle to house the prongs. Larger gauge probes are associated with a higher complication rate when placed in the liver. Intrahepatic hemorrhages and tumor seeding along the needle tract are more likely to occur [26].

The major contribution toward larger lesion size of bipolar ablation is based on a thermodynamic effect. If two lesions are

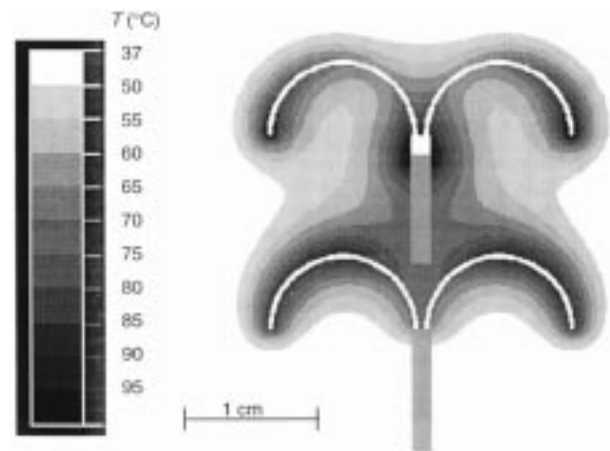


Fig. 10. Bipolar RF ablation: Temperature distribution after 12 min RF ablation in temperature-controlled mode, $T = 95 \text{ }^\circ\text{C}$. Only the prongs conduct current. The shafts (gray) are insulated, except for the distal 2 mm of the distal shaft. The outermost border (lightest gray) marks the $50 \text{ }^\circ\text{C}$ margin, which is considered the lesion border. Lesion size $V = 18.79 \text{ cm}^3$.

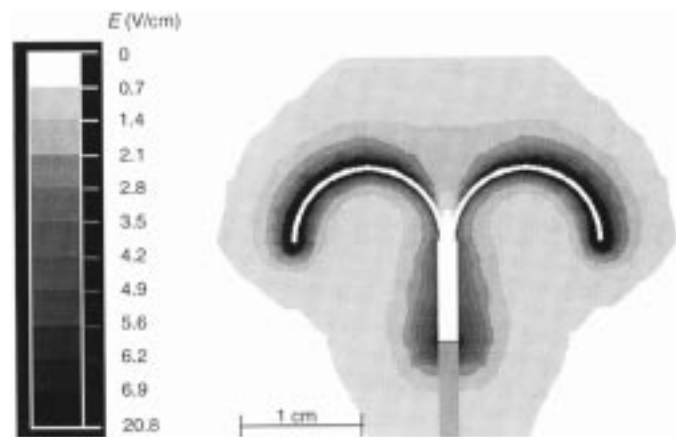


Fig. 11. Monopolar RF ablation: Electric field strength. The distal 10 mm of the shaft and the prongs conduct current. The gray part of the shaft is insulated.

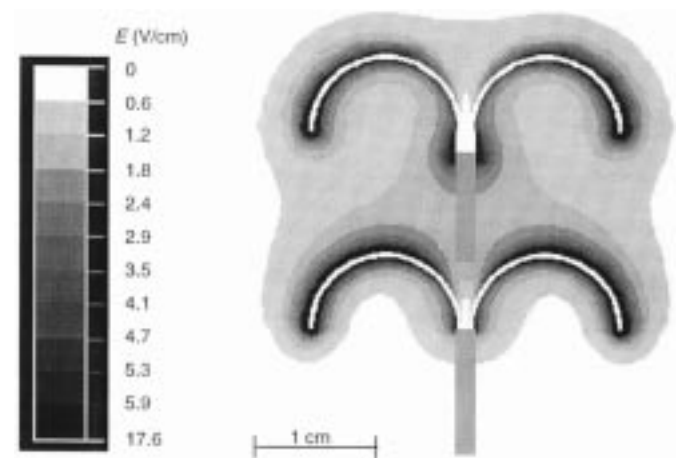


Fig. 12. Bipolar RF ablation: Electric field strength. The distal 2 mm of the distal probe shaft and the prongs of both probes conduct current. The gray parts of the shafts are insulated.

created separately with electrodes at the same position as in a bipolar ablation, the total lesion size is smaller than a single bipolar lesion. In monopolar ablation, heat is diverted from

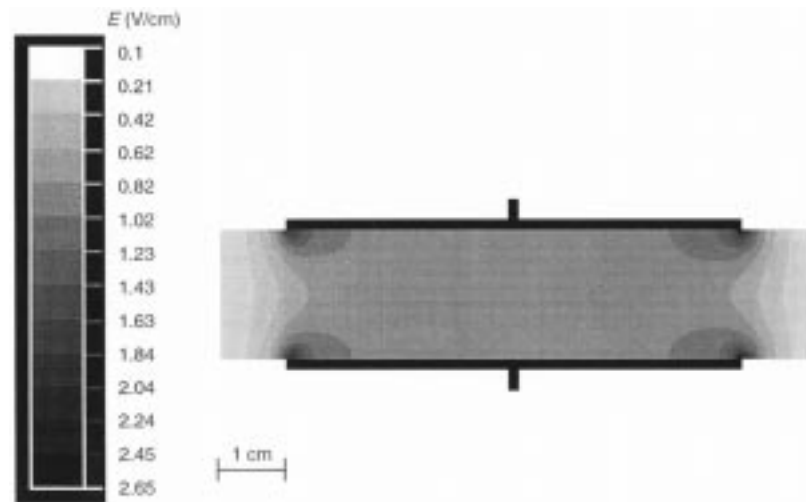


Fig. 13. Two parallel plates: electric field intensity. Homogenous electric field is created, except at the plate edges.

the ablation site in all directions. In the bipolar case, however, one probe is thermally shielded by the opposing second probe, which also actively heats the tissue in its proximity. There is less cooling in the direction toward the collateral probe than exists in monopolar ablation. Heat is trapped between the two probes and higher temperatures are reached. This results in a lesion of larger size than that of two lesions produced sequentially by monopolar ablation with probes placed at the same position. The temperature distributions for monopolar and bipolar ablation shown in Figs. 9 and 10 show increased lesion size between the probes in bipolar configuration. A zone of high temperature is created between the probes, which results in more effective killing of tumor cells in this zone. Furthermore, dependence of lesion size on local differences in cooling mediated by perfusion is reduced. This is supported by the fact that the standard deviation of bipolar ablation lesion size relative to its mean is smaller than for the monopolar case.

The average lesion size created *in vivo* with bipolar RF ablation ($V = 12.2 \pm 3 \text{ cm}^3$) was 210% larger than average lesion size of lesions created with monopolar RF ablation ($V = 3.9 \pm 1.8 \text{ cm}^3$). The results obtained from FEM analysis show only 136% increase of bipolar ($V = 18.79 \text{ cm}^3$) versus monopolar ($V = 7.95 \text{ cm}^3$). However, the conditions between the FEM model and the *in vivo* experiments have to be considered different. In the FEM model, we used temperature-independent tissue properties due to lack of data. We also considered blood perfusion to be constant whereas actually blood perfusion drops as coagulation occurs with high temperatures. Furthermore, we did not consider the impact of large blood vessels close to the ablation site. Due to these inaccuracies in the FEM model we obtain different results for the model and the experiment. However, both the FEM model and the *in vivo* experiments show a more than two-fold increase in lesion size, which demonstrates superior performance of the bipolar configuration.

Figs. 5 and 9 both show the typical mushroom shaped lesion observed after RF ablation utilizing umbrella probes. The lesion shape generated by bipolar ablation resembles a cylinder (see Figs. 6 and 10). It is easier to encompass tumors with a cylin-

drical bipolar lesion than with a mushroom shaped monopolar lesion.

McGahan *et al.* [16] made extensive bipolar RF ablation experiments *in vitro* using two needle electrodes. They found an ideal distance between the two needle electrodes. The situation is similar in our bipolar ablation method. When electrode distance is too far, two small, unfused lesions are generated instead of one large lesion. The sum of the small lesions in this case is smaller than the larger lesion created using a smaller gap. Since the intention is to kill a tumor located in between the electrodes, a continuous lesion between the electrodes has to be produced and, therefore, distance must be kept less than a certain limit. The liver is a very heterogeneous organ, particularly in regards to vascularity. Therefore, for the *in vivo* experiments there is no distance of probe spacing that is ideal for all cases. The ideal gap between the two probes depends upon the local properties of the ablation site and is different for each ablation. We performed preliminary *in vivo* experiments with probe distances of 3.5, 3, and 2.5 cm. When the distance was 3.5 and 3 cm, in some cases we found a gap of viable tissue between two lesions created by the two probes after performing ablation. We chose a distance of 2.5 cm for subsequent experiments. A different distance might be appropriate if hooked probes with other geometries are used (e.g., ten-prong umbrella probe from Radiotherapeutics, Sunnyvale, CA).

We rotated the probes 45° relative to each other to achieve more uniform current distribution and heating in between the probes. We did not perform any experiments to prove that this rotation is beneficial. We also insulated the distal 10 mm of the probe shafts. When probes are used for conventional monopolar ablation, the distal 10 mm of the shaft is not insulated and is electrically active (see Fig. 1). Initial experiments, where this section of the distal probe was not insulated, showed occurrences of charring around the distal portion of the shaft (see Fig. 7), which eventually resulted in impedance rise. Impedances above 200Ω trigger generator shut-down. This is a safety feature to avoid charring and boiling. An explanation for the rise in impedance is that the temperature at the uninsulated shaft exceeded the temperature monitored at the probe tips. The region around the

uninsulated shaft was heated more because it was closer to the second probe resulting in higher local current density. Temperatures above 100 °C cause boiling, vaporization and charring, which raises impedance. We solved this problem by insulating this region on the distal probe shaft using epoxy resin.

A limitation of the bipolar method described in this study is that temperature was measured at only one probe. In RF ablation, most of the active heating occurs within a range of a few millimeters from the electrodes. Similar resistivity and current density are present in the vicinity of both probes. Therefore, a comparable amount of energy is converted into heat next to each of the two probes. If one probe is cooled more by blood perfusion than the other, more heat energy is carried away. One probe reaches a higher temperature than the other. If the cooler probe is temperature-controlled at 95 °C, the uncontrolled probe reaches temperatures above 95 °C, which can lead to boiling and vaporization. Impedance rises, and the RF generator shuts down. In four cases, during bipolar ablation the impedance showed a sudden rise resulting in the shut-down of the generator. In these cases, we switched the connections of the probes so that the temperature of the previously overheating probe was measured. If the temperature of the hotter probe is controlled to be kept at 95 °C, the other probe does not reach this temperature and heating near this probe is less. Fig. 8 shows a lesion, where one probe produced only a minor lesion because the desired temperature was not reached.

When treating large tumors with current RF ablation techniques, multiple ablations often must be performed on the same tumor to obtain complete *necrosis* of tumor tissue. Bipolar RF ablation exhibited superior performance compared with monopolar ablation, creating lesions about three times as large in *in vivo* experiments. The proposed bipolar method may kill all tumor cells with a single application, which reduces treatment time. Since both probes can be inserted from the same site, insertion is only minimally more complicated compared with insertion of a single probe. Ultrasound guided placement can be used to place the probes on opposite sides of the tumor to be treated. Ultimately, a probe where two sets of electrodes at a specified distance are held within a single catheter could be manufactured. Different probes with variable distances between prong arrays, each specified for a certain tumor size, could be produced.

REFERENCES

- [1] M. C. Kew, "The development of hepatocellular carcinoma in humans," *Cancer Surv.*, vol. 5, pp. 719–739, 1985.
- [2] S. A. Curley, B. S. Davidson, R. Y. Fleming, F. Izzo, L. C. Stephens, P. Tinkey, and D. Cromens, "Laparoscopically guided bipolar radiofrequency ablation of areas of porcine liver," *Surg. Endosc.*, pp. 729–733, 1997.
- [3] W. Lounsbury, V. Goldschmidt, and C. Linke, "The early histologic changes following electrocoagulation," *Gastrointest. Endosc.*, vol. 41, pp. 68–70, 1995.
- [4] S. Rossi, M. Di Stasi, E. Buscarini, P. Quaretti, F. Garbagnati, L. Squasante, C. T. Paties, D. E. Silverman, and L. Buscarini, "Percutaneous RF interstitial thermal ablation in the treatment of hepatic cancer," *Amer. J. Roentgenol.*, vol. 167, pp. 759–768, 1996.
- [5] L. R. Jiao, P. D. Hansen, R. Havlik, R. R. Mitry, M. Pignatelli, and N. Habib, "Clinical short-term results of radiofrequency ablation in primary and secondary liver tumors," *Amer. J. Surgery*, vol. 177, pp. 303–306, 1999.
- [6] L. Solbiati, T. Ierace, S. N. Goldberg, S. Sironi, T. Livraghi, R. Fiocca, G. Servadio, G. Rizzatto, P. R. Mueller, A. Del Maschio, and G. S. Gazelle, "Percutaneous US-guided radiofrequency tissue ablation of liver metastases: Treatment and follow-up in 16 patients," *Radiology*, vol. 202, pp. 195–203, 1997.
- [7] S. A. Curley, F. Izzo, P. Delrio, L. M. Ellis, J. Granchi, P. Vallone, F. Fiore, S. Pignata, B. Daniele, and F. Cremona, "Radiofrequency ablation of unresectable primary and metastatic hepatic malignancies," *Ann. Surg.*, vol. 230, pp. 1–8, 1999.
- [8] S. N. Goldberg, G. S. Gazelle, L. Solbiati, W. J. Rittman, and P. R. Mueller, "Radio-frequency tissue ablation: Increased lesion diameter with a perfusion electrode," *Acad. Radiol.*, vol. 3, pp. 636–644, 1996.
- [9] T. A. Lorentzen, "A cooled needle electrode for radio-frequency tissue ablation: Thermodynamic aspects of improved performance compared with conventional needle design," *Acad. Radiol.*, vol. 3, pp. 556–563, 1996.
- [10] S. N. Goldberg, M. C. Stein, G. S. Gazelle, R. G. Sheiman, J. B. Kruskal, and M. E. Clouse, "Percutaneous radiofrequency tissue ablation: Optimization of pulsed-radiofrequency technique to increase coagulation necrosis," *J. Vasc. Interv. Radiol.*, vol. 10, pp. 907–916, 1999.
- [11] Y. Miao, Y. Ni, S. Mulier, K. Wang, M. F. Hoesz, P. Mulier, F. Penninckx, J. Yu, I. De Scheerder, A. L. Baert, and G. Marchal, "Ex vivo experiment on radiofrequency liver ablation with saline infusion through a screw-tip cannulated electrode," *J. Surg. Res.*, vol. 71, pp. 18–26, 1997.
- [12] R. S. Mittleman, S. K. Huang, W. T. De Guzman, H. Cuenoud, A. B. Wagshal, and L. A. Pires, "Use of saline infusion electrode catheter for improved energy delivery and increased lesion size in radiofrequency catheter ablation," *PACE*, vol. 18, pp. 1022–1027, 1995.
- [13] F. Burdio, A. Guemes, J. M. Burdio, T. Castiella, M. A. De Gregorio, R. Lozano, and T. Livraghi, "Hepatic lesion ablation with bipolar saline-enhanced radiofrequency in the audible spectrum," *Acad. Radiol.*, vol. 6, pp. 680–686, 1999.
- [14] E. Delva, Y. Camus, and B. Nordlinger, "Vascular occlusions for liver resections," *Ann. Surg.*, vol. 209, pp. 297–304, 1989.
- [15] S. N. Goldberg, P. F. Hahn, E. F. Halpern, R. M. Fogle, and G. S. Gazelle, "Radio-frequency tissue ablation: Effect of pharmacologic modulation of blood flow on coagulation diameter," *Radiology*, vol. 209, pp. 761–767, 1998.
- [16] J. P. McGahan, W.-Z. Gu, J. M. Brock, H. Tesluk, and C. D. Jones, "Hepatic ablation using bipolar radiofrequency electrocautery," *Acad. Radiol.*, vol. 3, pp. 418–422, 1996.
- [17] S. Tungjitkusolmun, E. J. Woo, H. Cao, J.-Z. Tsai, V. R. Vorperian, and J. G. Webster, "Thermal-electrical finite element modeling for radio frequency cardiac ablation: Effects of changes in myocardial properties," *Med. Biol. Eng. Comput.*, vol. 38, pp. 562–568, Sept. 2000.
- [18] —, "Finite element analyses of uniform current density electrodes for radio-frequency cardiac ablation," *IEEE Trans. Biomed. Eng.*, vol. 47, pp. 32–40, Jan 2000.
- [19] M. G. Curley and P. S. Hamilton, "Creation of large thermal lesions in liver using saline-enhanced RF ablation," in *Proc. 19th Annu. Int. Conf. IEEE Eng. Med. Biol. Soc. Piscataway, NJ, Chicago, 1997*, pp. 2516–2519.
- [20] H. Arkin, L. X. Xu, and K. R. Holmes, "Recent developments in modeling heat transfer in blood perfused tissues," *IEEE Trans. Biomed. Eng.*, vol. 41, pp. 97–107, Feb. 1994.
- [21] E. S. Ebbini, S.-I. Umemura, M. Ibbini, and C. A. Cain, "A cylindrical-section ultrasound phased-array applicator for hyperthermia cancer therapy," *IEEE Trans. Biomed. Eng.*, vol. 35, pp. 561–572, Sept. 1988.
- [22] D. Panescu, J. G. Whayne, S. D. Fleischman, M. S. Mirotznik, D. K. Swanson, and J. G. Webster, "Three-dimensional finite element analysis of current density and temperature distributions during radio-frequency ablation," *IEEE Trans. Biomed. Eng.*, vol. 42, pp. 879–890, Sept. 1995.
- [23] J. W. Valvano, J. R. Cochran, and K. R. Diller, "Thermal conductivity and diffusivity of biomaterials measured with self-heating thermistors," *Int. J. Thermophys.*, vol. 6, pp. 301–311, 1985.
- [24] H. H. Pennes, "Analysis of tissue and arterial blood temperatures in resting forearm," *J. Appl. Phys.*, vol. 1, pp. 93–122, 1948.
- [25] C. H. Cha, F. T. Lee, and J. M. Gurney, *et al.*, "CT versus sonography for monitoring radiofrequency ablation in a porcine liver," *Amer. J. Roentgenol.*, vol. 3, pp. 705–711, 2000.
- [26] G. D. Dodd, M. C. Soulen, and R. A. Kane *et al.*, "Minimally invasive treatment of malignant hepatic tumors: At the threshold of a major breakthrough," *Radiographics*, vol. 20, pp. 9–27, 2000.



Dieter Haemmerich (S'00) was born in Vienna, Austria on May 22, 1971. He received the B.S.E.E. degree from the Technical University of Vienna, Vienna, Austria, in 1997 and the M.S.B.M.E. degree from the University of Wisconsin, Madison, in 2000. He is currently working toward the Ph.D. degree in the Department of Biomedical Engineering, University of Wisconsin, Madison.

His research interests include finite element analysis of radio-frequency ablation and tissue impedance measurement.



S. Tyler Staelin, attended the University of Michigan, Ann Arbor, and Vanderbilt University School of Medicine, Nashville, TN, prior to training in surgery at the University of Wisconsin Hospital and Clinics, Madison, WI.

He is a Chief Resident in Surgery at the University of Wisconsin Hospital and Clinics, Madison.



Supan Tungjitsulmun (S'96-M'00) received the B.S.E.E. degree from the University of Pennsylvania, Philadelphia, in 1995, and the M.S.E.E. and Ph.D. degrees from the University of Wisconsin, Madison, in 1996, and 2000, respectively.

He is on the faculty of the Department of Electronics Engineering, King Mongkut's Institute of Technology-Ladkrabang, Bangkok, Thailand. His research interests include finite element modeling, and radio-frequency ablation. He is a contributing author to J. G. Webster (Ed.), *Design of Pulse Oximeters* (Bristol, U.K.: IOP, 1997). He is contributing author to J. G. Webster (Ed.), *Minimally Invasive Medical Technology* (Bristol, U.K.: IOP, 2001).

Dr. Tungjitsulmun is a member of Tau Beta Pi, Eta Kappa Nu, and Pi Mu Epsilon.



Fred T. Lee, Jr., received the B.A. and M.D. degrees from Boston University, Boston, MA, in 1984 and 1986, respectively.

After serving a residency in diagnostic radiology at The University of Rochester, he became a Faculty Member at the University of Wisconsin, Madison. He has been the Director of Abdominal Radiology since 2000. His research interests are in tumor ablation and radiographic contrast materials for the detection of cancer.



David M. Mahvi, received the B.S. degree in microbiology and premed from the University of Oklahoma, Norman, in 1977 and the M.D. degree from the University of South Carolina, Columbia, in 1981. He then completed the following postgraduate medical clinical training programs at Duke University: residency in surgery from 1981-1983; fellowship in immunology 1983-1985; residency in surgery 1985-1989.

In 1989, he joined the Section of Surgical Oncology, Department of Surgery at the University of Wisconsin-Madison where he is Professor of Surgery. He is Staff Surgeon, Oncologic and General Surgery, Middleton Memorial Veterans Hospital, Madison, WI; Member, University of Wisconsin Comprehensive Cancer Center; Permanent Member, Subcommittee F, Manpower and Training Study Section, National Institutes of Health, National Cancer Institute; General Surgery Residency Program Director, Department of Surgery, University of Wisconsin-Madison. His research interests include comparisons of treatment for patients with colorectal and other cancers using radio-frequency ablation, cryoablation, interferon alpha, interleukin-2, particle-mediated gene transfer, and toremifene.



John G. Webster (M'59-SM'69-F'86-LF'97) received the B.E.E. degree from Cornell University, Ithaca, NY, in 1953, and the M.S.E.E. and Ph.D. degrees from the University of Rochester, Rochester, NY, in 1965 and 1967, respectively.

He is Professor of Biomedical Engineering at the University of Wisconsin-Madison. In the field of medical instrumentation he teaches undergraduate and graduate courses, and does research on RF cardiac catheter ablation.

He is author of *Transducers and Sensors, An IEEE/EAB Individual Learning Program* (Piscataway, NJ: IEEE, 1989). He is coauthor, with B. Jacobson, of *Medicine and Clinical Engineering* (Englewood Cliffs, NJ: Prentice-Hall, 1977), and with R. Pallás-Areny, of *Sensors and Signal Conditioning*, 2nd edition (New York: Wiley, 2001) and with R. Pallás-Areny, of *Analog Signal Processing* (New York: Wiley, 1999). He is editor of *Encyclopedia of Medical Devices and Instrumentation* (New York: Wiley, 1988), *Tactile Sensors for Robotics and Medicine* (New York: Wiley, 1988), *Electrical Impedance Tomography* (Bristol, U.K.: Adam Hilger, 1990), *Teaching Design in Electrical Engineering* (Piscataway, NJ: Educational Activities Board, IEEE, 1990), *Prevention of Pressure Sores: Engineering and Clinical Aspects* (Bristol, U.K.: Adam Hilger, 1991), *Design of Cardiac Pacemakers* (Piscataway, NJ: IEEE Press, 1995), *Design of Pulse Oximeters* (Bristol, UK: IOP Publishing, 1997), *Medical Instrumentation: Application and Design*, Third Edition (New York: Wiley, 1998), *Handbook of Measurement, Instrumentation, and Sensors* (Boca Raton, FL: CRC, 1999), *Encyclopedia of Electrical and Electronics Engineering* (New York: Wiley, 1999), *Mechanical Variables Measurement* (Boca Raton, FL: CRC, 2000), and *Minimally Invasive Medical Technology* (Bristol, U.K.: IOP, 2001). He is coeditor, with A. M. Cook, of *Clinical Engineering: Principles and Practices* (Englewood Cliffs, NJ: Prentice-Hall, 1979) and *Therapeutic Medical Devices: Application and Design* (Englewood Cliffs, NJ: Prentice-Hall, 1982), with W. J. Tompkins, of *Design of Microcomputer-Based Medical Instrumentation* (Englewood Cliffs, NJ: Prentice-Hall, 1981) and *Interfacing Sensors to the IBM PC* (Englewood Cliffs, NJ: Prentice Hall, 1988), and with A. M. Cook, W. J. Tompkins, and G. C. Vanderheiden, of *Electronic Devices for Rehabilitation* (London, U.K.: Chapman & Hall, 1985).

Dr. Webster has been a member of the IEEE-EMBS Administrative Committee and the NIH Surgery and Bioengineering Study Section. He is a fellow of the Instrument Society of America, the American Institute of Medical and Biological Engineering, and the Institute of Physics. He is the recipient of the AAMI Foundation Laufman-Greatbatch Prize, the ASEE/Biomedical Engineering Division, Theo C. Pilkington Outstanding Educator Award and the ASEE/Engineering Libraries Division, Best Reference Work Award.